IEEE Access
Multidisciplinary | Rapid Review | Open Access Journal

Date of publication xxxx 00, 0000, date of current version xxxx 00, 0000.

Digital Object Identifier 10.1109/ACCESS.2017.DOI

Distributed Event-triggered Circular Formation Control for Multiple Anonymous Mobile Robots with Order Preservation and Obstacle Avoidance

PENG XU[1], WENXIANG LI[1], JIN TAO[2, 3], (Member, IEEE), MATTHIAS DEHMER[4, 5], Frank Emmert-Streib[6, 7], GUANGMING XIE[3], (Member, IEEE), MINYI XU[1] and QUAN ZHOU[2], (Member, IEEE)

[1]Marine Engineering College, Dalian Maritime University, Dalian 116026, China
[2]Department of Electrical Engineering and Automation, Aalto University, Espoo 02150, Finland
[3]College of Engineering, Peking University, Beijing 100871, China
[4]Swiss Distance University of Applied Science, Brig 3900, Switzerland
[5]College of Artificial Intelligence, Nankai University, Tianjin 300071, China
[6]Predictive Medicine and Data Analytics Lab, Department of Signal Processing,Tampere University of Technology, Tampere 33720, Finland
[7]Institute of Biosciences and Medical Technology, Tampere 33520, Finland

Corresponding author: Jin Tao (jin.tao@aalto.fi) and Mingyi Xu (xuminyi@dlmu.edu.cn).

The work was supported by the National Natural Science Foundation of China (Grant Nos. 51879022, 91648120, 61633002, 51575005, 61503008), the Beijing Natural Science Foundation (Grant No. 4192026), the Fundamental Research Funds for the Central Universities (Grant Nos. 3132019037 and 3132019197), the China Postdoctoral Science Foundation (Grant no. 2020M670045) and the Academy of Finland (Grant No. 315660).

ABSTRACT This paper investigates circular formation control problems for a group of anonymous mobile robots in the plane, where all robots can converge asymptotically to a predefined circular orbit around a fixed target point without collision, and maintain any desired relative distances from their neighbors. Given the limited resources for communication and computation of robots, a distributed event-triggered method is firstly designed to reduce dependence on resources in multi-robot systems, where the controller's action is determined by whether the norm of the event-trigger function exceeds zero through continuous sampling. And then, to further minimize communications costs, a self-triggered strategy is proposed, which only uses discrete states sampled and sent by neighboring robots at their event instants. Furthermore, for the two proposed control laws, a Lyapunov functional is constructed, which allows sufficient stability conditions to be obtained on the circular formation for multi-robot systems. And at the same time, the controllers are proved to exclude Zeno behavior. At last, numerical simulation of controlling uniform and non-uniform circular formations by two control methods are conducted. Simulation results show that the designed controller can control all mobile robots to form either a uniform circular formation or a non-uniform circular formation while maintaining any desired relative distances between robots and guaranteeing that there is no collision during the whole evolution. One of the essential features of the proposed control methods is that they reduce the update rates of controllers and the communication frequency between robots. And also, the spatial order of robots is also preserved throughout the evaluation of the system without collision.

INDEX TERMS Multi-robot System, Circular Formation, Event-triggered, Self-triggered, Directed Network

I. INTRODUCTION

In recent years, the control of multi-robot systems (MRSs) has gained increasing attention due to their wide applications, such as source localization [1], [2], pursuit and evasion [3] and surveillance [4]–[6], as well as theoretical challenges arising from the limitation in implementations. Formation control for MRSs aiming to drive multiple mobile robots to form and maintain a predetermined geometry has been actively studied [7]–[12]. In these studies, robots can move towards the desired location while maintaining specific

geometries through collaboration [13], [14]. By forming desired patterns, the robots can complete tasks with improved quality of the collected data and better robustness against adverse environmental interferences [15]. However, practical implementations of robots often have limited computational and communication capabilities, while tasks become increasingly complex. Therefore, it is highly desirable to design algorithms that can effectively utilize the communication medium's throughput capacity and robots' computing resources.

Event-triggered control mechanisms can replace commonly used periodic sampling, and consequently reduce the costs of computation, communication, and actuator effort, while maintaining the required performance [16]–[18], [21]–[26]. For first-order MRSs, event-triggered control methods have been actively studied for distributed formation control. For example, both centralized and distributed event-triggered control methods were designed to achieve consensus [17]. By utilizing sampled data instead of continuous data, a periodic event-based control framework was proposed for designing consensus protocols [18]. [19] addressed the circular formation problems with limited communication bandwidth using an encoder-decoder strategy. [20] further considered the scenario when the agents are under communication and computation constraints. Note that in [19], [20], all the robots were restricted to move in the 1-D space of a circle. For second-order MRSs, a distributed event-triggered control algorithm was proposed to reach consensus [21]. To further reduce computation resources and communication costs, an event-triggered control protocol based on the random sampling data and an improved time-dependent threshold was developed for the consensus of second-order multi-agent systems [22].

Forming circular formations is one of the most actively studied topics within the realm of formation control. On the one hand, circle formations are one of the simplest classes of formations with geometric shapes, and on the other hand, they are natural choices of the geometric shapes for a group of robots to exploit an area of interest. The circular formation problems can be classified into two essential tasks, target circling and spacing adjustment [27], [28]. The target circling aims to drive all robots to converge onto a circle around the target, while spacing adjustment aims to adjust all agents to reach the desired angular distance between pairs of neighboring robots. For example, [29] dealt with the situation that the mobile robots are subject to locomotion constraints. A limit-cycle-based decoupled-design approach was proposed to the circular formation problem [30], where each agent is modeled as a kinematic point and can merely obtain the relative positions of the target and its limited neighbors. For promoting the more general formation framework to establish, [31] studied a general formation problem for a group of mobile robots in a plane, in which the robots are required to maintain a distribution pattern, as well as to rotate around or remain static relative to a static/moving target. Moreover, event-triggered control has been widely applied to control the movement of robots in one-dimensional (1-D) space [19]–[22], [32]. However, few studies have been conducted for circular formation via event-triggered control in 2-D space, i.e., in the plane.

In our work, each robot, similar to Pioneer 3-DX [35], perceives the relative position of the target and the distance between the robot and its nearest counterclockwise neighbor through communication, while the neighbor robot will sense information in a clockwise direction. The main contributions of this paper are listed as follows. Firstly, a distributed event-triggered control method is designed to solve the circular formation control problems for MRSs. Secondly, a self-triggered strategy is proposed to further reduce the number of control actions and the amount of communication between neighbors without a significant performance reduction. In fact, the self-triggered control strategy is a class of special event-triggered control. The self-triggered strategy only uses the discrete states sampled and sent by neighbors at their event instants, such that continuous communication is avoided. Thirdly, Lyapunov functions are constructed, that allows to derive a sufficient stability condition on circular formation for MRSs. Our theoretical analysis and numerical simulations show that the proposed control methods can drive all mobile robots to converge to desired expected equilibrium points. Additionally, our results show that Zeno behavior, which is a phenomenon in hybrid systems that is of special interest, and it exists when an infinite number of discrete transitions occur in a finite time interval, can be avoided. The differences between this paper and previous works lie in:

(i) Different from previous works [19], [20], [29]–[31], the main goal of this paper is to design distributed event-triggered control laws that can guide a group of anonymous mobile robots with restricted computation and communication ability to form any given circular formation.
(ii) Different from [33] paying attention to incorporating an initial trajectory generator with the gradient-based inner optimizer, the main objective of this paper is to provide the conditions of order preservation guarantees collision avoidance in our problem setting.
(iii) Different from [34] addressing the highly constrained, nonlinear, and high-dimensional autonomous vehicle overtaking maneuver planning problem with an enhanced multiobjective particle swarm optimization, a more concise form of obstacle avoidance condition is provided to solve the circular formation problems for first-order dynamics MASs.

The remainder of this paper is organized as follows. In Section II, the preliminary definitions and the problem formulation are presented. A distributed event-triggered circle formation control law for a first-order system is designed, and the rigorous analysis of its performance is provided in Section III. Section IV addresses a self-triggered circle formation problem without continuous monitoring of the state of neighbors. Simulation results are given in Section V to validate the theoretical analysis. Section VI concludes the

This article has been accepted for publication in a future issue of this journal, but has not been fully edited. Content may change prior to final publication. Citation information: DOI 10.1109/ACCESS.2020.3023374, IEEE Access

paper and indicates possible extensions.

II. PRELIMINARIES AND PROBLEM STATEMENT

This section first lays down the notions and basic concepts from algebraic graph theory, then formulate the circular formation problem for multiple autonomous mobile robots in the plane.

A. PRELIMINARIES

The following two lemmas are used in our theoretical analysis. Lemma 1 is introduced to verify stability of the entire system. Due to each agent is described by a kinematic point, the interaction network between agents is described by a directed graph using algebraic graph theory. Lemma 2, which describes the properties of the directed graph, is required to perform further theoretical analysis. The notations used throughout this paper are listed in Table 1.

Lemma 1. *([36]) For any $x, y \in \mathbb{R}$ and $a > 0$, the following two properties are applied*

$$\begin{aligned} &1) \quad xy \le \frac{a}{2}x^2 + \frac{1}{2a}y^2, \\ &2) \quad (x^2+y^2) \le (x+y)^2, if \quad xy \ge 0. \end{aligned} \tag{1}$$

Lemma 2. *([37]) Given a directed graph $\mathcal{G}$, composed of spanning trees, the vector $\xi = [\xi_1, \xi_2, \ldots, \xi_N]^T > 0$ satisfies $\sum_{i=1}^{N} \xi_i = 1$ and $\xi^T \mathcal{L} = 0_N$, in which ξ denotes the left eigenvector corresponding to zero eigenvalue of the Laplacian matrix $\mathcal{L}$. Furthermore, $\mathcal{L}^T\Theta + \Theta\mathcal{L}^T$ is semi-positive definite where $\Theta = \mathrm{diag}\{\xi_1, \xi_2, \ldots, \xi_N\}$. After taking square root of each element of Θ, we obtain $\Upsilon = \mathrm{diag}\{\gamma_1, \gamma_2, \ldots, \gamma_N\}$, where $\gamma_i = \sqrt{\xi_i}, i = 1, \ldots, N$.*

TABLE 1: Notations.

Notations	Definations
$\mathbb{R}$	the set of real numbers
I_N	$N \times N$ identity matrix
A, $\|A\|$, A^T	matrix A, the Euclidean norm of A, the transpose of A
$1_N, 0_N$	N dimension column vectors with all entries equal to 1 and 0
$\mathrm{diag}\{a_1, a_2, \ldots, a_N\}$	the diagonal matrix with diagonal elements $a_1, a_2, \ldots, a_N$
$\mathcal{G}$	a directed graph composed of spanning trees
p_i, p_0	the mobile robot i, the predefined target point
u_i	the control input of robot i
$\hat{p}_i$	the position of robot p_i relative to the target point p_0
$\tilde{p}_i, \tilde{p}_{i^-}$	the position of robot p_i relative to its neighbor p_{i^+} and p_{i^-}
α_i, α_{i^-}	the angle between robot p_i and robot p_{i^+} and p_{i^-}
$\alpha_i^*, \alpha_{i^-}^*$	the desired angle from robot p_i to robot p_{i^+} and p_{i^-}
r	the radius of the desired circular formation

B. PROBLEM FORMULATION

Suppose in an obstacle-free plane, there exists N mobile robots $p = (p_1, p_2, \ldots, p_N)$ and the predefined target p_0 that to be circle around, as shown in Fig. 1. Here, each robot is anonymous and cannot recognize one from another and can move freely in the plane. The initial position of each robot is randomly generated and is not required to be distinguished from each other, whereas no robots occupy the same position with the target. For simplicity, the robots are labeled based on their initial positions according to the following three rules [30].

1) The labels are sorted in ascending order counterclockwise around the target.
2) For a robot located on the same ray extending from the target, its label is sorted in ascending order from the distance to the target point.
3) For robots occupying the same position, their labels will be randomly selected.

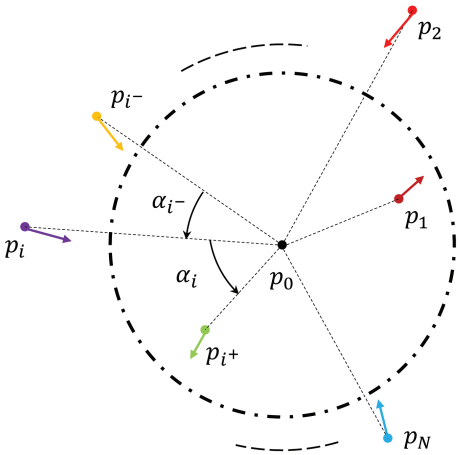

FIGURE 1: N robots are initially located in the plane.

Then, the robots' neighbor relationships are modeled by a directed graph $\mathcal{G} = (\mathcal{V}, \mathcal{E}, \mathcal{A})$, where $\mathcal{V} = \{p_1, p_2, \ldots, p_N\}$ denotes a group of mobile robots, $\mathcal{E} = \mathcal{V} \times \mathcal{V}$ is a set of communication edges that connects pairs of robots, and $\mathcal{A} = [a_{ij}] \in \mathbb{R}^{N \times N}$ denotes a weighted adjacency matrix.

In this relationship, each robot has only two adjacent neighbors, i.e., in front of or behind itself, marked as $\mathcal{N}_i = \{i^-, i^+\}$, where

$$i^+ = \begin{cases} i+1, & i = 1, 2, \ldots, N-1, \\ 1, & i = N, \end{cases} \tag{2}$$

and

$$i^- = \begin{cases} N, & i = 1, \\ i-1, & i = 2, 3, \ldots, N. \end{cases} \tag{3}$$

Let $p_i(t) = [x_i(t), y_i(t)]^T \in \mathbb{R}^2$ be the position of robot p_i at the time t, and $p_0 = [x_0, y_0]^T \in \mathbb{R}^2$ be the predefined target point. Therefore, robot p_i is modeled by a kinematic point

$$\dot{p}_i(t) = u_i(t), \quad i = 1, 2, \ldots, N, \tag{4}$$

where $u_i \in \mathbb{R}^2$ is the control input of robot p_i to be designed.

This article has been accepted for publication in a future issue of this journal, but has not been fully edited. Content may change prior to final publication. Citation information: DOI 10.1109/ACCESS.2020.3023374, IEEE Access

Suppose that each robot can only use the relative positions between the target and its two neighbors under the neighbor relationship $\mathcal{G}$, and it is worth noting that robots do not know the label information. The following notations are introduced to formulate the problem, as shown in Fig. 2.

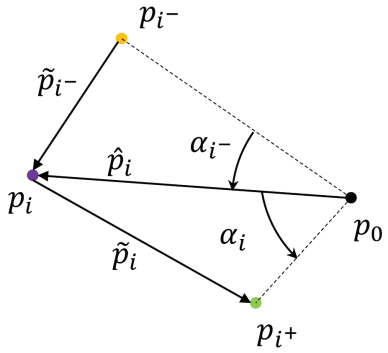

FIGURE 2: Relative positions and angles of robot p_i and its neighbors.

Let

$$\hat{p}_i(t) = p_i(t) - p_0, \quad i = 1, 2, \ldots, N. \tag{5}$$

be the position of robot p_i relative to the target point p_0.

The position of robot p_i relative to its neighbor p_{i^+} is expressed as

$$\tilde{p}_i(t) = p_{i^+}(t) - p_i(t), \quad i = 1, 2, \ldots, N. \tag{6}$$

The angle between robot p_i and robot p_{i^+} is described as

$$\alpha_i(t) = \angle p_i p_0 p_{i^+}, \quad i = 1, 2, \ldots, N.. \tag{7}$$

Let α_i^* represent the desired angle from robot p_i to its neighbor robot p_{i^+}, the desired angle of N robots is determined by the vector

$$\alpha_i^* = [\alpha_1^*, \alpha_2^*, \ldots, \alpha_N^*]^T. \tag{8}$$

Similarly, refers to (6), (7) and (8), the definations of robot p_i and robot p_{i^-} are written as

$$\begin{aligned} &\tilde{p}_{i^-}(t) = p_{i^-}(t) - p_i(t), \\ &\alpha_{i^-}(t) = \angle p_i p_0 p_{i^-}, \\ &\alpha_{i^-}^* = [\alpha_{1^-}^*, \alpha_{2^-}^*, \ldots, \alpha_{N^-}^*]^T. \end{aligned} \tag{9}$$

It is worth noting that there exists the desired radius $r > 0$, $\alpha_i^* > 0$ and $\sum_{i=1}^N \alpha_i^* = 2\pi$ such that the desired circular formation is admissible, where r is the radius of the desired circular formation.

Furthermore, to provide the N anonymous robots' initial states with their labels combined with the mathematical descriptions, the following definitions of the robots' spatial ordering are proposed.

Definition 1. *(Counterclockwise Order) The N robots are indicated to be arranged in a counterclockwise order if $\alpha_i \in (0, 2\pi)$ for all $i = 1, 2, \ldots, N$ and $\sum_{i=1}^N = \alpha_i = 2\pi$.*

Definition 2. *(Almost Counterclockwise Order) The N robots are indicated to be arranged in an almost counterclockwise order if 1) $\alpha_i \in [0, 2\pi)$ for all $i = 1, 2, \ldots, N$ and $\sum_{i=1}^N = \alpha_i = 2\pi$; and 2) when $\alpha_i = 0$, $\|\hat{p}_{i^+}\| > \|\hat{p}_i\|$.*

The definition of the circular formation problem is described as follows.

Definition 3. *(Circular Formation Problem) Given an admissible circular formation in the plane characterized by α^* and r, a distributed control protocol $u_i(t, \alpha^*, r, \hat{p}_i(t), \tilde{p}_i(t), \tilde{p}_{i^-}(t)), i = 1, 2, \ldots, N$ is designed such that the solution to the MRS (4) converges to some equilibrium points under any initial conditions, namely,*

$$\|\hat{p}_i\| = r, \quad i = 1, 2, \ldots, N, (Target \quad radius) \tag{10}$$

and

$$\alpha_i = \alpha_i^*, \quad i = 1, 2, \ldots, N, (Spacing \quad adjustment) \tag{11}$$

are satisfied.

Moreover, the desired properties of circular formation control for MRSs are presented as follows.

Definition 4. *(Order Preservation) For an MRS with N robots, under the control law $u_i(t)$, the robots' spatial ordering is maintained if N robots are initially located in an almost counterclockwise order in the plane. The solution to the MRS (4) can guarantee N robots maintain in a counterclockwise order, for all $t > 0$.*

Definition 5. *(Collision Avoidance) For an MRS with N robots, under the control law $u_i(t)$, the robots have the property of collision avoidance if N robots are initially arranged in an almost counterclockwise order in the plane. The solution to the MRS (4) satisfies $\|p_i\| - \|p_j\| > 0$ for any pair of i, j $(i \neq j)$, for all $t > 0$.*

III. EVENT-TRIGGERED CONTROL STRATEGY

Given a sampled-date protocol designed in [30], given as

$$u_i(t) = \varphi \begin{bmatrix} k_r l_i(t) & -1 \\ 1 & k_r l_i(t) \end{bmatrix} \hat{p}_i(t) g_i(t), i = 1, 2, \ldots, N, \tag{12}$$

where $\varphi > 0$, $k_r > 0$ are constant. $l_i(t) = r^2 - \|\hat{p}_i(t)\|$ and

$$g_i(t) = 1 + \frac{1}{2\pi} \left[\frac{\alpha_{i^-}^*}{\alpha_i^* + \alpha_{i^-}^*} \alpha_i(t) - \frac{\alpha_i^*}{\alpha_i^* + \alpha_{i^-}^*} \alpha_{i^-}(t) \right]. \tag{13}$$

From (13), the variable α_i can be treated as an additional state of the MRS. It is known that each robot has to transmit a request continuously to its neighbors for acquiring their additional states, and then calculate $g_i(t)$ and $l_i(t)$. However, in reality, the communication and computing capabilities of robots usually have limitations, which makes the control law (12) unable to be implemented in practice.

In order to address this issue, an event-triggered strategy is proposed based on the addition states, in which

This article has been accepted for publication in a future issue of this journal, but has not been fully edited. Content may change prior to final publication. Citation information: DOI 10.1109/ACCESS.2020.3023374, IEEE Access

computations of $g_i(t)$ and $l_i(t)$ are only conducted at discrete event instants. Therefore, undesirable transmission and computation can be avoided. Let an increasing sequence $(t_0^i, t_1^i, \ldots, t_k^i, \ldots)$ denote the event instants of robot p_i, such that $\alpha_i(t_k^i)$ is the state of of robot p_i at the k-th event instants. Note that due to all robots trigger asynchronously and have their own event sequences. Then, the control law based on the event-triggered scheme is designed as

$$u_i(t) = \varphi \begin{bmatrix} k_r l_i(t_i^k) & -1 \\ 1 & k_r l_i(t_i^k) \end{bmatrix} \hat{p}_i(t) g_i(t_i^k), t \in (t_i^k, t_i^{k+1}]. \tag{14}$$

Substituting (12) into (4), the closed-loop dynamics of robot p_i is presented as

$$\dot{p}_i(t) = \varphi \begin{bmatrix} k_r l_i(t_i^k) & -1 \\ 1 & k_r l_i(t_i^k) \end{bmatrix} \hat{p}_i(t) g_i(t_i^k), i = 1, 2, \ldots, N. \tag{15}$$

By $\hat{p}_i(t)$, (15) can be rearanged as

$$\dot{\hat{p}}_i(t) = \varphi \begin{bmatrix} k_r l_i(t_i^k) & -1 \\ 1 & k_r l_i(t_i^k) \end{bmatrix} \hat{p}_i(t) g_i(t_i^k), i = 1, 2, \ldots, N. \tag{16}$$

Moreover, from (7), we have

$$\dot{\tilde{\alpha}}_i(t) = \dot{\tilde{\alpha}}_{i^+}(t_i^k) - \dot{\tilde{\alpha}}_i(t_i^k), \quad i = 1, 2, \ldots, N, \tag{17}$$

where $\tilde{\alpha}_i(t_i^k)$ denotes the angle of the vector $\hat{p}_i(t_i^k)$.

Then,

$$\begin{aligned} &\dot{\tilde{\alpha}}_i(t_i^k) = \varphi g_i(t_i^k), \\ &\|\dot{\hat{p}}_i(t_i^k)\| = k_r \varphi \|\hat{p}_i(t_i^k)\|(r^2 - \|\hat{p}_i(t_i^k)\|^2) g_i(t_i^k). \end{aligned} \tag{18}$$

Substituting (18) into (17), the dynamical equation of the additional states combined with the event-triggered strategy is obtained as

$$\dot{\alpha}_i(t) = \varphi(g_{i^+}(t_k^i) - g_i(t_k^i)), t \in [t_k^i, t_{k+1}^i), \tag{19}$$

Assuming that $\hat{\alpha}_i(t) = \alpha_i(t_k^i)$, $\delta_i(t) = \alpha_i(t)/\alpha_i^*$, $\hat{\delta}_i(t) = \hat{\alpha}_i(t)/\alpha_i^*$, (19) can be rearranged as

$$\begin{aligned} \alpha_i^* \dot{\delta}_i(t) = \frac{\varphi}{2\pi} \Bigg(&\left[\frac{\alpha_i^*}{\alpha_{i^+}^* + \alpha_i^*} \hat{\alpha}_{i^+}(t) - \frac{\alpha_{i^+}^*}{\alpha_{i^+}^* + \alpha_i^*} \hat{\alpha}_i(t) \right] - \\ &\left[\frac{\alpha_{i^-}^*}{\alpha_i^* + \alpha_{i^-}^*} \hat{\alpha}_i(t) - \frac{\alpha_i^*}{\alpha_i^* + \alpha_{i^-}^*} \hat{\alpha}_{i^-}(t) \right] \Bigg). \end{aligned} \tag{20}$$

Using δ_i, (20) can be summarized into a simple form as

$$\dot{\delta}_i(t) = \frac{\varphi}{2\pi} \sum_{j \in \mathcal{N}_i} \frac{\alpha_j^*}{\alpha_i^* + \alpha_j^*} \left(\hat{\delta}_j(t) - \hat{\delta}_i(t) \right), t \geq 0. \tag{21}$$

A deviation variable is defined as $e_i(t) = \hat{\delta}_i(t) - \delta_i(t)$. Then a compact form of the system dynamics can be derived as

$$\dot{\delta}(t) = -\frac{\varphi}{2\pi} L_d^T (\delta(t) + e(t)), t \in [t_k^i, t_{k+1}^i), \tag{22}$$

where $\delta(t) = [\delta_1(t), \delta_2(t), \ldots, \delta_N(t)] \in \mathbb{R}^N$, and $e(t) = [e_1(t), e_2(t), \ldots, e_N(t)] \in \mathbb{R}^N$.

For the dynamical equation (19), the event-triggered circular formation control for MRSs can be solved by Theorem 2.

Theorem 1. *Given any admissible circular formations characterized by α^* and r, considering the MRS (4) and the designed control law (14) over a strongly connected weight unbalanced digraph $\mathcal{G}$, the circular formation problem is solvable when the event-trigger condition designs as*

$$f_i(t) = \|e_i(t)\| - \frac{\sigma \|\gamma_i \bar{\delta}_i(t)\|}{\|\Upsilon L_d^T\| \rho \mathbf{e}^{\|l_i(t)\|}}, 0 < \sigma < 1, \tag{23}$$

where $\rho > 1$, $\bar{\delta}_i(t)$ is the i-th elements of $\bar{\delta}(t) = [\bar{\delta}_1(t), \bar{\delta}_2(t), \ldots, \bar{\delta}_N(t)]^T \triangleq L_d^T \delta(t)$, Υ is the same diagonal matrix as described in Lemma 2, γ_i is the i-th diagonal element of matrix Υ.

Furthermore, in the MRS (4), there exists at least one robot $m \in \mathcal{V}$ for which the next inter-event interval is strictly positive under event-triggered condition (23).

Proof:

A Lyapunov function candidate is considered as

$$V(t) = \frac{1}{4} \delta^T(t) (L_d \Theta + \Theta L_d^T) \delta(t), \tag{24}$$

where Θ is the same diagonal matrix as in Lemma 2, such that $L_d \Theta + \Theta L_d^T$ is semi-positive definite.

As a result, $\dot{V}(t) \leq 0$ and $V(t) = 0$ if the circular formation problem is solvable. Then, the derivative of the Lyapunov function (24) along with the trajectories of the MRS yields to

$$\begin{aligned} \dot{V}(t) &= \delta^T(t) L_d \Theta (-\frac{\varphi}{2\pi} L_d^T (\delta(t) + e(t))) \\ &= -\frac{\varphi}{2\pi} \delta^T(t) L_d \Theta L_d^T \delta(t) - \frac{\varphi}{2\pi} \delta^T(t) L_d \Theta L_d^T e(t) \\ &\leq -\frac{\varphi}{2\pi} \|\Upsilon L_d^T \delta(t)\|^2 + \frac{\varphi}{2\pi} \|\Upsilon L_d^T \delta(t)\| \|\Upsilon L_d^T e(t)\| \rho \mathbf{e}^{\|l_i(t)\|}, \end{aligned} \tag{25}$$

Enforcing the event condition (23), we obtain that $\|e_i(t)\| \leq \frac{\sigma \|\gamma_i \bar{\delta}_i(t)\|}{\|\Upsilon L_d^T\| \rho \mathbf{e}^{\|l_i(t)\|}}$. Subsequently, $\rho \mathbf{e}^{\|l_i(t)\|} \|\Upsilon L_d^T e(t)\| \leq \rho \mathbf{e}^{\|l_i(t)\|} \|\Upsilon L_d^T\| \|e(t)\| \leq \sigma \|\Upsilon L_d^T \delta(t)\|$. Then, (25) is rearranged into

$$\begin{aligned} \dot{V}(t) &\leq \frac{\varphi}{2\pi} \|\Upsilon L_d^T \delta(t)\|^2 (\sigma - 1) \\ &\leq \frac{\varphi}{2\pi} \|\Upsilon \bar{\delta}(t)\|^2 (\sigma - 1). \end{aligned} \tag{26}$$

As $0 < \sigma < 1$, we obtain that $\dot{V}(t) \leq 0$ and $\dot{V}(t) = 0$ if the circular formation problem is solvable.

In the following, the realization of the desired addition state is explained in detail.

Since the graph $\mathcal{G} = (\mathcal{V}, \mathcal{E}, \mathcal{A})$ is strongly connected, we have

$$\lim_{t \to \infty} \delta(t) = c \mathbf{1}_N \tag{27}$$

where $c > 0$ is a constant.

This article has been accepted for publication in a future issue of this journal, but has not been fully edited. Content may change prior to final publication. Citation information: DOI 10.1109/ACCESS.2020.3023374, IEEE Access

$$L_d = \begin{bmatrix} \frac{\alpha_2^*}{\alpha_2^*+\alpha_1^*} + \frac{\alpha_N^*}{\alpha_N^*+\alpha_1^*} & -\frac{\alpha_1^*}{\alpha_2^*+\alpha_1^*} & 0 & \cdots & 0 & -\frac{\alpha_1^*}{\alpha_N^*+\alpha_1^*} \\ -\frac{\alpha_2^*}{\alpha_2^*+\alpha_1^*} & \frac{\alpha_3^*}{\alpha_3^*+\alpha_2^*} + \frac{\alpha_1^*}{\alpha_2^*+\alpha_1^*} & -\frac{\alpha_2^*}{\alpha_3^*+\alpha_2^*} & \cdots & 0 & 0 \\ \vdots & \vdots & \vdots & \vdots & \vdots & \vdots \\ 0 & 0 & 0 & \cdots & \frac{\alpha_N^*}{\alpha_N^*+\alpha_{N-1}^*} + \frac{\alpha_{N-2}^*}{\alpha_{N-1}^*+\alpha_{N-2}^*} & -\frac{\alpha_{N-1}^*}{\alpha_N^*+\alpha_{N-1}^*} \\ -\frac{\alpha_N^*}{\alpha_N^*+\alpha_1^*} & 0 & 0 & \cdots & -\frac{\alpha_N^*}{\alpha_N^*+\alpha_{N-1}^*} & \frac{\alpha_1^*}{\alpha_N^*+\alpha_1^*} + \frac{\alpha_{N-1}^*}{\alpha_N^*+\alpha_{N-1}^*} \end{bmatrix},$$

By the definition of $\delta(t)$, we have

$$\lim_{t\to\infty} \alpha(t) = c\alpha^* \tag{28}$$

Note that $\alpha_i(t)$ satisfies $\sum_{i=1}^N \alpha_i = 2\pi$ for all $t \geq 0$, and $\alpha_i^*(t)$ satisfies $\sum_{i=1}^N \alpha_i^* = 2\pi$, we derive $c = 1$. More precisely,

$$\lim_{t\to\infty} \alpha(t) = \alpha^*.$$

This result indicates that the desired addition states can be achieved by all robots.

Further, an estimate of the positive lower bound on the inter-event times is proved. It is easy to obtain that for robot p_i, the event interval between t_{k+1}^i and t_k^i is the period $\frac{\|e_i(t)\|}{\gamma_i\bar{\delta}_i(t)}$, which increases from 0 to $\frac{\sigma}{\|\Upsilon L_d^T\|\rho\mathbf{e}^{\|l_i(t)\|}}$. Define $m = \arg\max_{i\in\mathcal{V}} \|\gamma_i\bar{\delta}_i(t)\|$, robot m stands for maximum the maximum norm of $\gamma_i\bar{\delta}_i(t)$ among all the robots, which implies

$$\frac{\|e_m(t)\|}{\|\gamma_m\bar{\delta}_m(t)\|} \leq \frac{\|e(t)\|}{\|\gamma_m\bar{\delta}_m(t)\|} \leq \frac{\sqrt{N}\|e(t)\|}{\|\Upsilon\bar{\delta}(t)\|}. \tag{29}$$

From (29), the time $\frac{\|e_m(t)\|}{\|\gamma_m\bar{\delta}_m(t)\|}$ attains $\frac{\sigma}{\|\Upsilon L_d^T\|\rho\mathbf{e}^{\|l_i(t)\|}}$ is longer than $\frac{\sqrt{N}\|e(t)\|}{\|\Upsilon\bar{\delta}(t)\|}$ costs. That is, $\tau_m > \tau$, where τ_m represents positive interval $(t_{k+1}^m - t_k^m)$ is lower bounded, and τ is the time $\frac{\|e(t)\|}{\|\Upsilon\bar{\delta}(t)\|}$ increasing from 0 to $\frac{\sigma}{\sqrt{N}\|\Upsilon L_d^T\|\rho\mathbf{e}^{\|l_i(t)\|}}$. Thereby, the time derivative of $\frac{\|e(t)\|}{\|\Upsilon\bar{\delta}(t)\|}$ is written as (30).

Let β stand for $\frac{\|e(t)\|}{\|\Upsilon\bar{\delta}(t)\|}$, then, $\dot{\beta} \leq \frac{\varphi}{2\pi}\|\Upsilon^{-1}\|(1 + \|\Upsilon L_d^T\|\beta)^2$. Here, $\beta \leq \epsilon(t,\epsilon_0)$, where $\epsilon(t,\epsilon_0)$ is the solution of $\dot{\epsilon}(t,\epsilon_0) = \frac{\varphi}{2\pi}\|\Upsilon^{-1}\|(1 + \|\Upsilon L_d^T\|\alpha(t,\alpha_0))^2$, and $\epsilon(0,\epsilon_0) = \epsilon_0$.

According to

$$\frac{2\pi d\epsilon}{\varphi\|\Upsilon^{-1}\|(1 + \|\Upsilon L_d^T\|\epsilon(t,\epsilon_0))^2} = dt, \tag{31}$$

we can see that the interval between event instants t_k and t_{k+1} is lower bounded by the interval τ which satisfies $\epsilon(\tau,0) = \frac{\sigma}{\|\Upsilon L_d^T\|\rho\mathbf{e}^{\|l_i(t)\|}}$. By solving (31), we have

$$\begin{aligned} \tau &= \frac{2\pi\epsilon(\tau,0)}{\varphi\|\Upsilon^{-1}\|(1 + \|\Upsilon L_d^T\|\epsilon(\tau,0))} \\ &= \frac{2\pi\sigma}{\varphi(\rho\mathbf{e}^{\|l_i(t)\|} + \sigma)\|\Upsilon L_d^T\|\|\Upsilon^{-1}\|}. \end{aligned} \tag{32}$$

From (32), we obtain

$$\tau' = \frac{2\pi\sigma}{\varphi(\sqrt{N}\rho\mathbf{e}^{\|l_i(t)\|} + \sigma)\|\Upsilon L_d^T\|\|\Upsilon^{-1}\|},$$

where τ' is the time $\frac{\|e(t)\|}{\|\Upsilon\bar{\delta}(t)\|}$ ranging from 0 to $\frac{\sigma}{\sqrt{N}\|\Upsilon L_d^T\|\rho\mathbf{e}^{\|l_i(t)\|}}$.

The minimal interval between two event instants of robot m can be written as

$$\tau_m = \frac{2\pi\sigma}{\varphi(\sqrt{N}\rho\mathbf{e}^{\|l_i(t)\|} + \sigma)\|\Upsilon L_d^T\|\|\Upsilon^{-1}\|}. \tag{33}$$

From $\tau_m > 0$, we draw a conclusion that there exists at least one robot $m \in \mathcal{N}$ in the MRS (4), which prevents the occurrence of Zeno behavior under the event-trigger condition (23).

IV. SELF-TRIGGERED CONTROL STRATEGY

The event-triggered solution, earlier discussed in Section III, assumes continuous communication among the neighboring robots. In this section, a self-triggered strategy, which is a special class of event-triggered control, is applied to minimize communications costs further. Namely, the self-triggered strategy only uses the discrete states that are sampled and sent by neighbors at their own event instants.

For the designed dynamical equation (19), the self-triggered circular formation control for the distributed MRSs is solved by Theorem 2.

Theorem 2. *Given any admissible circular formations characterized by α^* and r, and considering the MRS (4) and the designed control law (14) over a strongly connected weight-unbalanced digraph $\mathcal{G}$, the circular formation problem is solvable when the event-triggered condition is designed as*

$$\tilde{f}_i(t) = \|e_i(t)\| - \frac{\|L_d^T(i,j)\hat{\delta}(t)\|}{(b+1)\|L_d^T\|\rho\mathbf{e}^{\|l_i(t)\|}}, b > 0, \tag{34}$$

where $L_d^T(i,j)\hat{\delta}(t) = \sum_{j\in\mathcal{N}_i} L_d^T(i,j)(\hat{\delta}_i(t) - \hat{\delta}_j(t))$.

And the condition

$$-\xi_i + \frac{\xi_i^2}{2a} + \frac{b+1}{b^3(t)M} > 0, i = 1,2,\ldots,N, \tag{35}$$

holds simultaneously, where $M = \min\{\rho\mathbf{e}^{\|l_i(t)\|}\}$. Moreover, the self-trigger condition (34) helps the MRS (4) to avoid the occurrence of Zeno behavior.

Proof:

This article has been accepted for publication in a future issue of this journal, but has not been fully edited. Content may change prior to final publication. Citation information: DOI 10.1109/ACCESS.2020.3023374, IEEE Access

$$\begin{aligned}\frac{d}{dt}\frac{\|e(t)\|}{\|\Upsilon\bar{\delta}(t)\|} &= \frac{d}{dt}\frac{(e(t)^Te(t))^{1/2}}{(\bar{\delta}^T(t)\Upsilon\Upsilon\bar{\delta}(t))^{1/2}}\\ &= \frac{e(t)\dot{e}(t)}{\|e(t)\|\|\Upsilon\bar{\delta}(t)\|} - \frac{\bar{\delta}^T(t)\Upsilon\Upsilon\dot{\bar{\delta}}(t)\|e(t)\|}{\|\Upsilon\bar{\delta}(t)\|^3}\\ &= \frac{-\varphi e(t)\Upsilon^{-1}\Upsilon(\bar{\delta}(t)+L_d^Te(t))}{2\pi\|e(t)\|\|\Upsilon\bar{\delta}(t)\|} - \frac{\varphi\bar{\delta}^T(t)\Upsilon\Upsilon L_d^T(\bar{\delta}(t)+L_d^Te(t))\|e(t)\|}{2\pi\|\Upsilon\bar{\delta}(t)\|^2\|\Upsilon\bar{\delta}(t)\|}\\ &\le \frac{\varphi\|\Upsilon^{-1}\|(\|\Upsilon\bar{\delta}(t)\|+\|\Upsilon L_d^Te(t))\|}{2\pi\|\Upsilon\bar{\delta}(t)\|} + \frac{\varphi\|\Upsilon L_d^T\|\|\Upsilon^{-1}\|(\|\Upsilon\bar{\delta}(t)\|+\|\Upsilon L_d^Te(t)\|)\|e(t)\|}{2\pi\|\Upsilon\bar{\delta}(t)(t)\|^2}\\ &\le \frac{\varphi\|\Upsilon\|}{2\pi}\left(1+\frac{\|e(t)\|\|\Upsilon L_d^T\|\|\Upsilon\bar{\delta}(t)\|}{\|\Upsilon\bar{\delta}(t)\|}\right)^2.\end{aligned} \tag{30}$$

A Lyapunov function candidate is considered as

$$V(t) = \frac{1}{4}\delta^T(t)(L_d\Theta+\Theta L_d^T)\delta(t), \tag{36}$$

As a result, $V(t) > 0$ and $V(t) = 0$ if the circular formation problem is solvable. Then the derivative of the Lyapunov function along of the trajectories of the MRS (4) yields to

$$\begin{aligned}\dot{V}(t) &= \delta^T(t)L_d\Theta(-\frac{\varphi}{2\pi}L_d^T(\delta(t)+e(t)))\\ &= -\frac{\varphi}{2\pi}\delta^T(t)L_d\Theta L_d^T\delta(t) - \frac{\varphi}{2\pi}\delta^T(t)L_d\Theta L_d^Te(t).\end{aligned} \tag{37}$$

From Lemma 1, there exists $\delta^T(t)L_d\Theta L_d^Te(t) \le \frac{1}{2a}\delta^T(t)L_d\Theta^2L_d^T\delta(t) + \frac{a}{2}e^T(t)L_dL_d^Te(t)$ such that (37) is rearranged into

$$\begin{aligned}\dot{V}(t) \le &-\frac{\varphi}{2\pi}\delta^T(t)L_d\Theta L_d^T\delta(t)+\\ &\frac{\varphi}{2\pi}(\frac{1}{2a}\delta^T(t)L_d\Theta^2L_d^T\delta(t)+\frac{a}{2}e^T(t)L_dL_d^Te(t)).\end{aligned} \tag{38}$$

In the following, we explain the analytical relationship between $\delta^T(t)L_dL_d^T\delta(t)$ and $e^T(t)L_dL_d^Te(t)$.

From the designed self-trigger condition (34), we have

$$L_d^Te(t) \le \|L_d^T\|\|e(t)\| \le \frac{\|L_d^T\hat{\delta}(t)\|}{(b+1)\rho\mathbf{e}^{\|l_i(t)\|}}. \tag{39}$$

Together with the definition of e_i and (39), it yields to

$$\begin{aligned}e^T(t)L_dL_d^Te(t) \le &\frac{1}{(b+1)^2\rho^2\mathbf{e}^{2\|l_i(t)\|}}\\ &\left((\delta(t)+e(t))^TL_dL_d^T(\delta(t)+e(t))\right)\\ \le &\frac{1}{(b+1)^2\rho^2\mathbf{e}^{2\|l_i(t)\|}}\left(\delta(t)^TL_dL_d^T\delta(t)+\right.\\ &\left.(.e(t)^TL_dL_d^Te(t)+2\delta(t)^TL_dL_d^Te(t))\right)\\ \le &\frac{1}{(b+1)^2\rho^2\mathbf{e}^{2\|l_i(t)\|}}(1+\frac{1}{b})\delta(t)^TL_dL_d^T\delta(t)\\ &+\frac{1+2b}{(b+1)^2\rho^2\mathbf{e}^{2\|l_i(t)\|}}e(t)^TL_dL_d^Te(t).\end{aligned} \tag{40}$$

Thus,

$$e^T(t)L_dL_d^Te(t) \le \frac{b+1}{b^3(t)M}\delta(t)^TL_dL_d^T\delta(t). \tag{41}$$

Substituting (41) into (38), we have

$$\begin{aligned}\dot{V}(t) &\le -\frac{\varphi}{2\pi}\delta^T(t)L_d\Theta L_d^T\delta(t) + \frac{\varphi}{2\pi}(\frac{1}{2a}\delta^T(t)L_d\Theta^2L_d^T\delta(t)\\ &\quad+\frac{b+1}{b^3(t)M}\delta(t)^TL_dL_d^T\delta(t))\\ &\le -\frac{\varphi}{2\pi}\sum_{i=1}^{N}(-\xi_i+\frac{\xi_i^2}{2a}+\frac{b+1}{b^3(t)M})\|\bar{\delta}_i\|.\end{aligned} \tag{42}$$

Therefore, the condition (34) guarantees $\dot{V}(t) < 0$ and $\dot{V}(t) = 0$ if the circular formation problem is solvable.

To avoid Zeno behavior, an estimate of the positive lower bound on the inter-event times is further proved. Assuming that the $k+1$th event of robot p_i occurs at the time $t_k^i+\tau_i$, we derives $\|e_i(t_k^i)\| = 0$, and

$$\|e_i(t_k^i+\tau_i)\| = \frac{\|L_d^T(i,j)\hat{\delta}(t)\|}{(b+1)\|L_d^T\|\rho\mathbf{e}^{\|l_i(t)\|}}. \tag{43}$$

From the trajectory of $e_i(t)$, we have

$$\begin{aligned}\|e_i(t_k^i+\tau_i)\| &= \left\|\int_{t_k^i}^{t_k^i+\tau_i}\dot{e}_i(t)dt\right\|\\ &= \left\|\int_{t_k^i}^{t_k^i+\tau_i}\dot{\delta}_i(t)dt\right\|\\ &= \left\|\int_{t_k^i}^{t_k^i+\tau_i}\frac{\varphi}{2\pi}L_d^T(i,j)\hat{\delta}(t)dt\right\|\\ &\le \frac{\varphi}{2\pi}\|L_d^T(i,j)\hat{\delta}(t)\|\tau\end{aligned} \tag{44}$$

Substituting (43) into (44), we get

$$\frac{\|L_d^T(i,j)\hat{\delta}(t)\|}{(b+1)\|L_d^T\|\rho\mathbf{e}^{\|l_i(t)\|}} \le \frac{\varphi}{2\pi}\|L_d^T(i,j)\hat{\delta}(t)\|\tau, \tag{45}$$

where $\tau = \frac{2\pi}{\varphi(b+1)\|L_d^T\|\rho\mathbf{e}^{\|l_i(t)\|}} \ge 0$.

To sum up, if a neighbour triggers during the interval between two consecutive events of robot p_i, that is, the

This article has been accepted for publication in a future issue of this journal, but has not been fully edited. Content may change prior to final publication. Citation information: DOI 10.1109/ACCESS.2020.3023374, IEEE Access

neighbour triggers at time $t_k^i + \tau_j \leq t_k^i + \tau_i$. Then the interval is greater than τ_j. We conclude that the intervals between events that generated by the self-triggered function are positive.

V. NUMERICAL EXAMPLES

Considering an MRS, consisting of six mobile robots located in the plane, the target point is set to (0, 0), and the desired angle distances between each pair of neighboring robots are set to satisfy (8). Namely, the desired distribution pattern can be set arbitrarily as long as the coefficients of the designed controller make sure the condition holds. The initial positions of six robots are randomly generated.

To show the relative superiority of the event triggered strategy, the event detection of all those simulations is executed using a sampled-data approach. Here, $h = 0.01s$ is chosen as the sampling periods in real-time control. We choose the coefficients of the controller to make ensure the condition holds. To our best knowledge, the role of coefficients mentioned is to keep $l_i(t)$ remain at least an order of magnitude comparing to $g(t)$.

A. EXAMPLE OF EVENT-TRIGGERED FORMATION CONTROL

We first apply the event-triggered control strategy to the uniform circular formation control with the desired angle distance $\alpha_i^* = \pi/3$ and the desired radius of the circular formation $r = 100$. Using the proposed control law, the coefficients of which are set to $\varphi = 0.4$, $k_r = 0.002$ to satisfy the event-triggered condition (23), to solve the uniform circle formation problem and the simulation results are shown in Fig. 3. Fig. 3(a) reveals the trajectories of six robots in the plane, and Fig. 3(b) shows the difference between the event-triggered angled and the set angles, the distances difference between the event-triggered radius of the circular formation and the predefined radius, and the evolution of control laws of the six robots, respectively. We observe that the desired uniform circular formation can be achieved asymptotically under the designed control law. Furthermore, the average inter-event time for all robots is obtained as $h_{avg} = 0.0229$. Comparing to the sampling period h, we can observe that the average inter-event period h_{avg} has the advantages of reducing the amount of control update. Note that increasing σ can further reduce computation over the whole process, but will increase the cumulative error of the system, which leads to system uncertainties.

We then extend the method to the non-uniform circular formation, where the desired angle distance is set to $\alpha^* = [\pi/4, \pi/3, 3\pi/8, 7\pi/24, \pi/3, 5\pi/12]$. Furthermore, r, initial positions of robots, as well as the coefficients φ, k_r are set the same as the first case. The simulation results are shown in Fig. 4. Fig. 4(a) reveals the trajectories of six robots in the plane, and Fig. 4(b) shows the differences between the event-triggered angles and the set angles, the distances differences between the event-triggered radius of the circular formation and the predefined radius, and the evolution of control laws

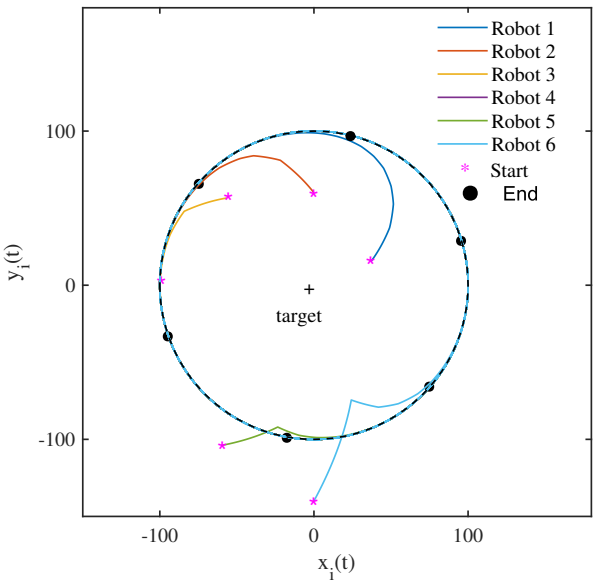

(a) The trajectories of six robots in the plane at $t \in (0, 200)$

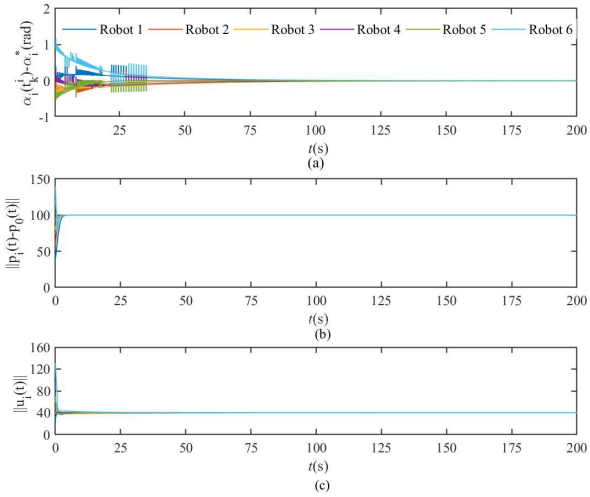

(b) The evolution of $\|\alpha_i(t_i^k) - \alpha_i^*\|$, $\|p_i(t_i^k) - p_0\|$, $\|u_i(t)\|$ for $i = 1, 2, \ldots, 6$

FIGURE 3: Uniform circular formation control via event-triggered strategy.

of the six robots, respectively. We can observe that compared to the convention circular formation control algorithm, as shown in Reference [30], due to the event-triggered strategy, trade-offs among actuator effort and computation would be reduced dramatically by as much as $1/3$ without increasing the computational complexity. For both uniform and non-uniform circular formation, the multiple robots under the control law (14) have the properties of order preservation and collision avoidance. It should be noted that compared with traditional protocols, the use of event-triggered control may introduce convergence errors.

This article has been accepted for publication in a future issue of this journal, but has not been fully edited. Content may change prior to final publication. Citation information: DOI 10.1109/ACCESS.2020.3023374, IEEE Access

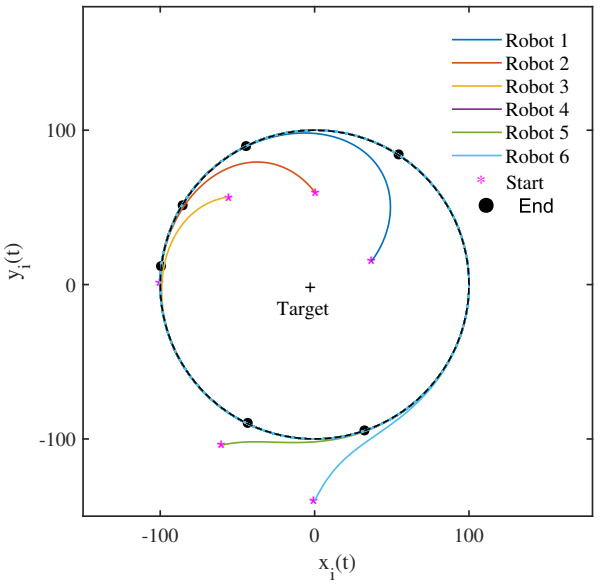

(a) The trajectories of six robots in the plane at $t \in (0, 200)$

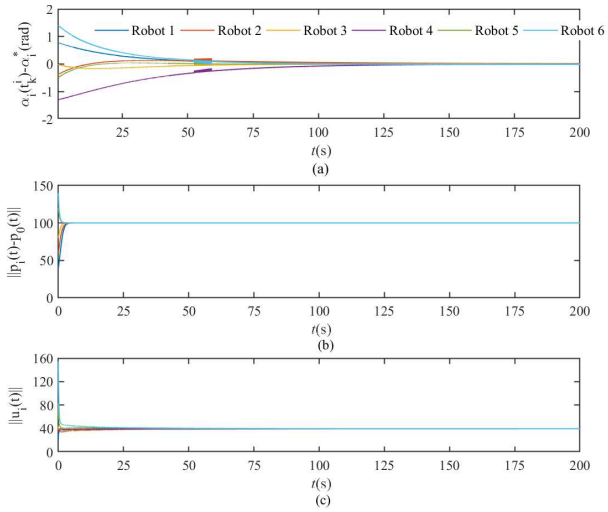

(b) The evolution of $\|\alpha_i(t_i^k) - \alpha_i^*\|$, $\|p_i(t_i^k) - p_0\|$, $\|u_i(t)\|$ for $i = 1, 2, \ldots, 6$

FIGURE 4: Non-uniform circular formation control via event-triggered strategy.

B. EXAMPLE OF SELF-TRIGGERED FORMATION CONTROL

The self-triggered control strategy is first applied to the uniform circular formation control with the desired angle distance $\alpha_i^* = \pi/3$ and the desired radius of the circular formation $r = 100$. Using the proposed control law, the coefficients of are set to $\varphi = 0.4$, $k_r = 0.002$ to satisfy the trigger function (34), to solve the uniform circle formation problem and the simulation results are shown in Fig. 5. Fig. 5(a) shows the trajectories of six robots in the plane, and Fig. 5(b) shows the difference between the event-triggered angled and the set angles, the difference of the distances between the event-triggered radius of the circular formation and the predefined radius, and the evolution of control laws of the six robots, respectively. We observe that the desired uniform circular formation can be achieved asymptotically under the designed self-triggered control law.

The self-triggered control strategy is also extended to the non-uniform circular formation problem, where the desired angle distance is set to $\alpha^* = [\pi/4, \pi/3, 3\pi/8, 7\pi/24, \pi/3, 5\pi/12]$. And r, initial positions of robots, as well as the coefficients φ, $k_r$are set the same as the previous case. The simulation results are shown in Fig. 6. Fig. 6(a) reveals the trajectories of six robots in the plane, and Fig. 6(b) shows the differences between the event-triggered angles and the set angles, the distances differences between the event-triggered radius of the circular formation and the predefined radius, and the evolution of control laws of the six robots, respectively. We can see that the desired non-uniform circular formation can be achieved asymptotically under the designed self-triggered control law. Comparing Fig. 4(b) with Fig. 6(b), we observe that under the self-triggered control with intermittent monitoring of measurement errors, the MRS can still achieve circular formation. Hence, the energy consumption of communication can be reduced under the designed self-triggered control law.

To further compare the performance between the event-triggered and self-triggered control strategies, the average inter-event period, the amount of computation, and data transmissions of each simulation case are listed in Table 2. We can see from Table 2 that in terms of the frequency of control updates, the result of the self-triggered method is more conservative than the event-triggered schemes. However, event-triggered control still requires continuous communication. The self-triggered control law is effective in reducing both data transmission and amounts of computation, in which the next triggered instance is predicted relied upon the last triggered data. Thus, we draw a conclusion that the proposed self-triggered control law is effective in reducing data transmission, and the control time changes very little. From a practical point of view, this is more straightforward to apply to resource-limited situations.

TABLE 2: Data Transmission Comparison.

Methods	Average inter-event period (s)	Number of computation times	Number of data transmission times
Event-triggered (uniform)	0.0229	8733	20000
Event-triggered (non-uniform)	0.0285	7017	20000
Self-triggered (uniform)	0.0155	12903	12903
Self-triggered (non-uniform)	0.0157	12738	12738

VI. CONCLUSION

This paper investigated the problem of controlling a group of anonymous mobile robots distributed in a circular formation.

This article has been accepted for publication in a future issue of this journal, but has not been fully edited. Content may change prior to final publication. Citation information: DOI 10.1109/ACCESS.2020.3023374, IEEE Access

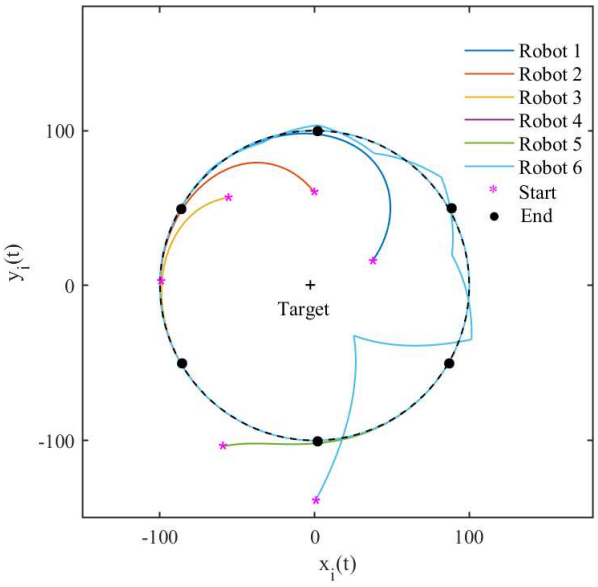

(a) The trajectories of six robots in the plane at $t \in (0, 200)$

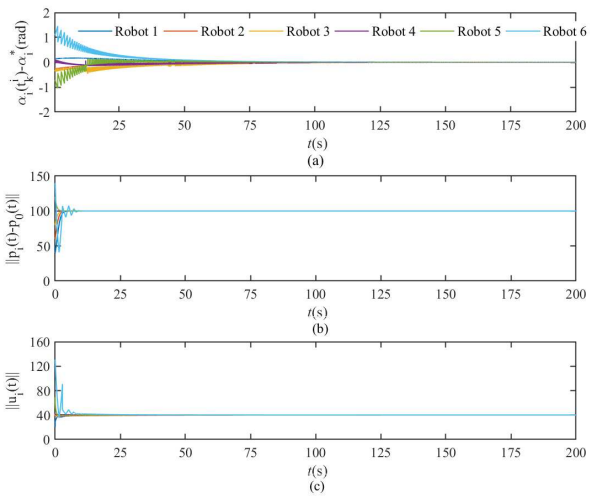

(b) The evolution of $\|\alpha_i(t_i^k) - \alpha_i^*\|$, $\|p_i(t_i^k) - p_0\|$, $\|u_i(t)\|$ for $i = 1, 2, \ldots, 6$

FIGURE 5: Uniform circular formation control via event-triggered strategy.

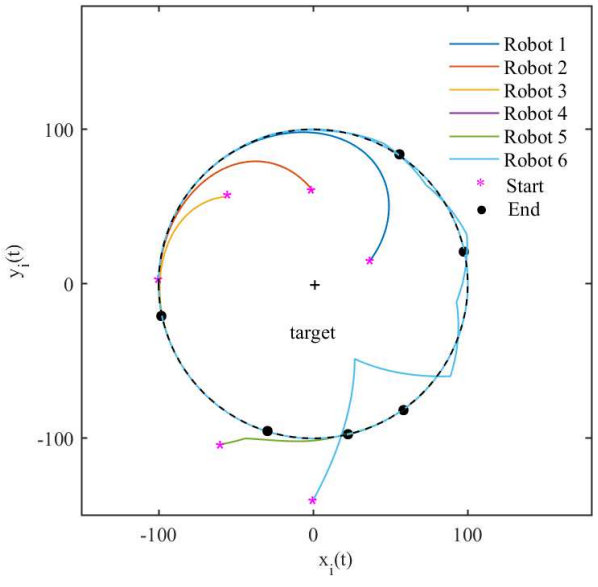

(a) The trajectories of six robots in the plane at $t \in (0, 200)$

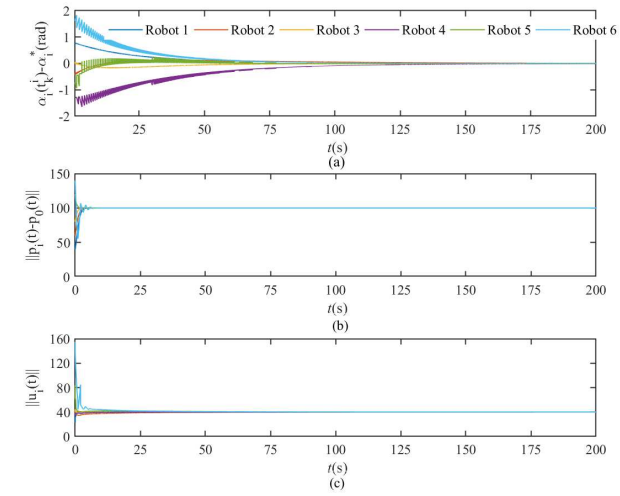

(b) The evolution of $\|\alpha_i(t_i^k) - \alpha_i^*\|$, $\|p_i(t_i^k) - p_0\|$, $\|u_i(t)\|$ for $i = 1, 2, \ldots, 6$

FIGURE 6: Non-uniform circular formation control via self-triggered strategy.

Given the robots' limited communication and computation resources, a distributed event-triggered algorithm was designed to reduce dependence on resources in MRSs. Through continuous sampling among the neighboring robots, the designed event-trigger controller judges whether the event trigger function's norm exceeds zero to determine the controller's update. To further minimize communications costs, a self-triggered strategy only uses the discrete states that sampled and sent by neighboring robots at their own event instants was proposed, which can reduce both the computation and the communication frequency between robots by up to 1/3. Moreover, theoretical analysis proved that the two proposed controllers could completely avoid Zeno behavior. At last, numerical simulation results of using two controllers to control uniform and non-uniform circular formations were given to verify the theoretical analysis. Future work will extend the proposed method in this paper to more complex systems, such as adding the influence of space-time topology or considering unreliable links in communication networks. Also, finding convincing comparison results is also one of the main focuses of our next work.

REFERENCES

[1] C. Dou, D. Yue, Q. L. Han, J. M. Guerrero, "Multi-agent system-based event-triggered hybrid control scheme for energy Internet," *IEEE Access*,

vol. 5, pp. 3263-3272, Feb. 2017.

[2] B. Sami, "Intelligent energy management for off-grid renewable hybrid system using multi-agent approach," *IEEE Access*, vol. 8, pp. 8681-8696, Jan. 2020.

[3] W. Ding, G. Yan, Z. Lin, "Pursuit formations with dynamic control gains," *Int. J. Robust Nonlinear Control*, vol. 22, pp. 300-317, Jan. 2011.

[4] J. Pav'n, J. G'omez-Sanz, A. Fern'andez-Caballero, J. Valencia-Jim'enez, "Development of intelligent multisensor surveillance systems with agents," *Robot. Auton. Syst.*, vol. 55, no. 12, pp. 892–903, Dec. 2007.

[5] G. Zhang, G. K. Fricke, D. P. Garg, "Spill detection and perimeter surveillance via distributed swarming agents," *IEEE-ASME Trans. Mechatron.*, vol. 18, no. 1, pp. 121–129, Feb. 2013.

[6] T. Ahmed, X. Wei, S. Ahmed, A. Pathan, "Efficient and effective automated surveillance agents using kernel tricks," *Simulation*, vol. 89, no. 5, pp. 562–577, Nov. 2012.

[7] X. Lu, F. Austin, S. Chen, Formation control for second-order multi-agent sys- tems with time-varying delays under directed topology, *Commun. Nonlinear Sci. Numer. Simul.*, vol. 17, no. 3, pp. 1382–1391, Mar. 2012.

[8] C. Wang, G. Xie, M. Cao, "Forming Circle Formations of Anonymous Mobile Agents With Order Preservation," *IEEE Trans. Autom. Control*, vol. 58, no. 12, pp. 3248-3254, Dec. 2013.

[9] D. Meng, K. L. Moore, "Learning to cooperate: Networks of formation agents with switching topologies," *Automatica*, vol. 64, pp. 278–293, Feb. 2016.

[10] H. Su, G. Y. Tang, "Rolling optimization formation control for multi-agent system- s under unknown prior desired shapes," *Inf. Sci.*, vol. 459, pp. 255–264, Aug. 2018.

[11] P. Xu, H. Zhao, G. Xie, J. Tao, M. Xu, "Pull-based distributed event-triggered circle formation control for multi-agent systems with directed topologies, " *Appl. Sci-Basel*, vol. 9, no. 23, pp. 4995, Nov. 2019.

[12] Z. Zhang, J. Hu, H. Huang, "Formation tracking for nonlinear uncertain multi-agent systems via adaptive output feedback quantized control," *IEEE Access*, vol. 7, pp. 95696 - 95709, Jul. 2019.

[13] W. Xia, M. Cao, Clustering in diffusively coupled networks," *Automatica*, vol. 47, no. 11, pp. 2395–2405, Nov. 2011.

[14] K. K. Oh, M. C. Park, H. S. Ahn, "A survey of multi-agent formation control," *Automatica*, vol. 53, pp. 424–440, Mar. 2015.

[15] F. Bullo, J. Cortes, S. Martinez, "Distributed control of robotic networks: a mathematical approach to motion coordination algorithms," Princeton University Press, 2009.

[16] J. Zhou, Y. H. Guo, G. Li , J. Zhang, "Event-triggered control for nonlinear uncertain second-order multi-agent formation with collision avoidance," *IEEE Access*, vol. 7, pp. 104489 - 104499, Jul. 2019.

[17] D. V. Dimarogonas, E. Frazzoli, K. H. Johansson, "Distributed event-triggered control for multi-agent systems," *IEEE Trans. Autom. Control*, vol. 57, no. 5, pp. 1291–1297, May. 2012.

[18] X. Meng, L. Xie, Y. C. Soh, "Asynchronous periodic event-triggered consensus for multi-agent systems," *Automatica*, vol. 84, pp. 214–220, Oct. 2017.

[19] P. Xu, J. Wen, C. Wang, G. Xie, "Distributed circle formation control over directed networks with communication constraints," *15th IFAC Symposium on Large Scale Complex Systems LSS 2019*, vol. 52, no. 3, pp. 108-113, May. 2019.

[20] J. Wen, P. Xu, C. Wang, G. Xie, Y. Gao, "Distributed event-triggered circle formation control for multi-agent systems with limited communication bandwidth," *Neurocomputing*, vol. 358, pp. 211–221, Sep. 2019.

[21] H. Yan, Y. Shen, H. Zhang, H. Shi, "Decentralized event-triggered consensus control for second-order multi-agent systems," *Neurocomputing*, vol. 133, pp. 18 – 24, Jun. 2014.

[22] N. Mu, X. Liao, T. Huang, "Consensus of second-order multi-agent systems with random sampling via event-triggered control," *J. Franklin Inst.*, vol. 353, no. 6, pp. 1423–1435, Apr. 2016.

[23] Q. Jia, W. K. Tang, "Consensus of multi-agents with event-based nonlinear cou- pling over time-varying digraphs," *IEEE Trans. Circuits Syst. II-Express Briefs*, vol. 65, no. 12, pp. 1969–1973, Jan. 2018.

[24] C. Jiang, H. Du, W. Zhu, L. Yin, X. Jin, G. Wen, "Synchronization of nonlinear networked agents under event-triggered control," *Inf. Sci.*, vol. 459, pp. 317–326, Aug. 2018.

[25] J. Liu, Y. Zhang, C. Sun, Y. Yu, "Fixed-time consensus of multi-agent systems with input delay and uncertain disturbances via event-triggered control," *Inf. Sci.*, vol. 480, pp. 261–272, Apr. 2019.

[26] J. Dai, G. Guo, "Event-triggered leader-following consensus for multi-agent sys- tems with semi-markov switching topologies," *Inf. Sci.*, vol. 459, pp. 290–301, Aug. 2018.

[27] X. Defago, A. Konagaya, " Circle formation for oblivious anonymous mobile robots with no common sense of orientation," *Proc. 2th ACM Int. workshop on Principles of mobile computing*, pp. 97–104, Oct. 2002.

[28] X. D'efago, S. Souissi, "Non-uniform circle formation algorithm for oblivious mobile robots with convergence toward uniformity," *Theor. Comput. Sci.*, vol. 396, no. 1-3, pp. 97–112, May. 2018.

[29] C. Wang, G. Xie, M. Cao, "Controlling anonymous mobile agents with unidirectional locomotion to form formations on a circle," *Automatica*, vol. 50, no. 4, pp. 1100-1108, Apr. 2014.

[30] C. Wang, G. Xie, "Limit-cycle-based decoupled design of circle formation control with collision avoidance for anonymous agents in a plane", *IEEE Trans. Autom. Control*, 2017, 62(12): 6560-6567.

[31] C. Wang, W. Xia, G. Xie, "Limit-cycle-based design of formation con- trol for mobile agents", *IEEE Trans. Autom. Control*,vol. 65, no. 8, pp. 3530 - 3543, Oct. 2019, .

[32] P. Xu, G. Xie, J. Tao, M. Xu, Q. Zhou, "Observer-based event-triggered circle formation control for first-and second-order multiagent systems", *Complexity*, vol. 2020, pp. 4715315, Mar. 2020.

[33] R. Chai, A. Tsourdos, A. Savvaris, S. Chai, Y. Xia, "Two-stage trajectory optimization for autonomous ground vehicles parking maneuver", *IEEE Trans. Ind. Electron.*, vol. 15, no. 7, pp. 3899 - 3909, Nov. 2018.

[34] R. Chai, A. Tsourdos, A. Savvaris, S. Chai, Y. Xia and C. L. P. Chen, "Multiobjective overtaking maneuver planning for autonomous ground vehicles," in *IEEE Trans. Cybern.*, Early access, March 2020. doi: 10.1109/TCYB.2020.2973748

[35] S. Zaman, W. Slany, G. Steinbauer, "ROS-based mapping, localization and autonomous navigation using a pioneer 3-dx robot and their relevant issues," *2011 Saudi International Electronics, Communications and Photonics Conference (SIECPC)*, pp. 1–5, Apr. 2011.

[36] A. Garsia, "On a convex function inequality for martingales," *The Annals of probability*, vol. 1, no. 1, pp. 171–174, 1973.

[37] W. Ren, R. Beard, "Consensus seeking in multiagent systems under dynamically changing interaction topologies", *IEEE Trans. Autom. Control*, vol. 50, no. 5, pp. 655–661, May. 2005.